
LASER-PLASMA INTERACTIONS IN LARGE GAS-FILLED HOHLRAUMS

R. E. Turner

R. L. Kauffman

T. D. Shepard

L. V. Powers

B. F. Lasinski

G. F. Stone

R. L. Berger

B. J. MacGowan

L. J. Suter

C. A. Back

D. S. Montgomery

E. A. Williams

D. H. Kalantar

D. H. Munro

Introduction

Indirect-drive targets planned for the National Ignition Facility (NIF) laser consist of spherical fuel capsules enclosed in cylindrical Au hohlraums. Laser beams, arranged in cylindrical rings, heat the inside of the Au wall to produce x rays that in turn heat and implode the capsule to produce fusion conditions in the fuel. Detailed calculations show that adequate implosion symmetry can be maintained by filling the hohlraum interior with low-density, low-Z gases.¹ The plasma produced from the heated gas provides sufficient pressure to keep the radiating Au surface from expanding excessively.

As the laser heats this gas, the gas becomes a relatively uniform plasma with small gradients in velocity and density. Such long-scale-length plasmas can be ideal mediums for stimulated Brillouin Scattering (SBS). SBS can reflect a large fraction of the incident laser light before it is absorbed by the hohlraum; therefore, it is undesirable in an inertial confinement fusion (ICF) target. To examine the importance of SBS in NIF targets, we used Nova to measure SBS from hohlraums with plasma conditions similar to those predicted for high-gain NIF targets. The plasmas differ from the more familiar exploding foil or solid targets as follows: they are hot (3 keV); they have high electron densities ($n_e = 10^{21}\text{cm}^{-3}$); and they are nearly stationary, confined within an Au cylinder, and uniform over large distances (>2 mm). These hohlraums have $<3\%$ peak SBS backscatter for an interaction beam with intensities of $1\text{--}4 \times 10^{15}\text{ W/cm}^2$, a laser wavelength of $0.351\text{ }\mu\text{m}$, $f/4$ or $f/8$ focusing optics, and a variety of beam smoothing implementations. Based on these conditions, we conclude that SBS does not appear to be a problem for NIF targets.

Theory

In the NIF targets, the laser beams will propagate through several millimeters of plasma ($n_e \sim 10^{21}\text{cm}^{-3}$) before depositing energy in the hohlraum wall. In this case, $n_e/n_c \sim 0.1$ for $0.351\text{-}\mu\text{m}$ light, where n_c is the critical density or the maximum density through which light of a given wavelength can propagate. The fraction of the laser energy that is collisionally absorbed in the low-Z (low atomic number) gas fill is modest ($\sim 10\%$ at the peak of the laser pulse). However, estimates based on simple linear gain theory generate concern that SBS reflectivities could exceed acceptable levels for the large-scale-length plasmas in these targets.

SBS is one of several parametric instabilities that can occur in a plasma. In the case of SBS, the laser light reflects off of an ion-acoustic wave in the plasma. A chain of events occur if certain resonance conditions are met: the size of the ion-acoustic wave increases, which causes the scattered light to increase, which causes the ion-acoustic wave to increase, etc., until nonlinear effects limit the process. SBS reflectivity $>10\%$ may unacceptably degrade target performance by reducing the energy available for radiation heating and/or by disrupting symmetry.

In the NIF plasmas, density and velocity gradients are weak (although they limited the growth region for SBS in previous experiments); however, damping of the SBS-produced ion waves by light ions in the gas fill is efficient² and limits the SBS gain coefficient. Predicted gain coefficients for NIF plasmas, using linear theory, are >20 , whereas gains of <15 are required to insure reflectivities of 10% or less. For such large gains, theoretical estimates³ indicate that nonlinear mechanisms will limit the scattering to lower levels. Because nonlinear damping is difficult to calculate, we must do experiments to verify these estimates. Previous SBS

experiments are insufficient, since the plasma conditions in past studies⁴ differ significantly from expected NIF conditions. For those exploding foil or solid targets, where scale lengths <1 mm and electron temperatures $T_e \sim 0.5$ – 2 keV were typical, SBS is limited by detuning (loss of phase matching conditions), due to gradients in the flow velocity. The lack of quantitative theoretical understanding of those experiments discourages extrapolation to NIF conditions. There is little data on the effect of various beam-smoothing techniques, or increased laser bandwidth, interacting with NIF-type plasmas.

Random phase plates (RPP)⁵ and temporal smoothing methods such as smoothing by spectral dispersion (SSD)⁶ are commonly used in laser-plasma interaction experiments to increase the time-averaged beam uniformity at the target plane. The idea is to avoid having higher-than-average intensities in the interaction region, since high intensities more easily drive SBS. Localized regions of higher intensity can occur because of imperfections in the laser beam. They can also occur when there is filamentation of the beam in the plasma. The filamentation instability has thresholds very similar to those for SBS, and can be initially seeded by imperfections in the laser beam. The smoothing techniques reduce the intensity variations in the beam but on a time scale that is often comparable to the SBS growth time. The interactions among SBS, filamentation, and the short-time-scale smoothed beam are complicated and not completely understood. One goal of these experiments is to test the f -number and temporal smoothing scale of SBS.

Instability growth in an RPP intensity distribution⁷ can vary with the size of the speckles. The role of speckles in determining instability levels is important for NIF because the underdense plasma size is large compared with the speckle length of the proposed $f/8$ beam focusing. In simulations,^{8,9} $f/8$ beams filament more than $f/4$ beams. Three-dimensional simulations¹⁰ show that SBS reflectivity, unlike filamentation, is not directly limited by the speckle length. In these simulations, SBS grows over the entire resonant region, which is several speckles long, with a total gain greater than that calculated for the average intensity. However, even if the bandwidth is less than the SBS growth rate, temporal smoothing reduces SBS by partially destroying the cooperative scattering among hot spots. Modification of the RPP intensity distribution by filamentation could also affect SBS. For the plasma parameters of these experiments and laser intensity $I \sim 2 \times 10^{15}$ W/cm², simulations indicate that $f/4$ speckles are stable to filament but $f/8$ speckles are unstable.⁹ Temporal smoothing makes filamentation more difficult because the filament must form rapidly, before the hot spot moves to a different location.

Experiment

We use the Nova laser to produce plasmas with conditions similar to those predicted for NIF hohlraum targets and to measure SBS from these plasmas. In these experiments, the targets are cylindrical Au hohlraums with a length and diameter of 2.5 mm.¹¹ The hohlraums do not contain capsules, but are filled with neopentane (C₅H₁₂) gas at a pressure of 1 atm ($n_e = 10^{21}$ cm⁻³ when fully ionized). For some targets, a trace of Ar is also added for diagnostic purposes. As shown in Fig. 1, the gas is contained by two polyimide (C₂₂H₁₀N₂O₅) windows ~ 6500 Å thick. Nine of Nova's beams are used to heat the gas with ~ 30 kJ of 0.351- μ m light in a 1.4-ns shaped pulse. The tenth beam is a probe, or interaction, beam whose intensity, pulse shape, f -number, and "smoothness" are varied. The SBS backscatter intensity and spectrum from the interaction beam are measured with temporal resolution of 100 ps and spectral resolution of 1 Å. The interaction beam has a trapezoidal pulse with a ~ 600 -ps flat top and a ~ 300 -ps rise and fall time. The interaction beam is typically delayed ~ 600 ps relative to starting the heating beams and is smoothed spatially with an RPP, providing peak average intensities in the range of 1 – 4×10^{15} W/cm². Temporal smoothing is done either by SSD with FM bandwidth⁶ or by four colors. (See "Four-Color Irradiation System for Laser-Plasma Interaction Experiments," p. 130 of this *Quarterly* for a discussion of four-color systems.) The four-color scheme propagates four different frequencies through four quadrants of the laser. The focusing lens overlaps the frequencies at the focal plane. The line separation is $\delta\lambda = 4.4$ Å at 1.053 μ m for a total line width of 13.2 Å for these experiments (four-color bandwidth with $\delta\lambda \cong 10$ Å is proposed for the NIF).

To produce a uniformly hot plasma inside the Nova hohlraum, a substantial fraction of Nova's energy (~ 12 kJ) must be coupled to the gas. Because the

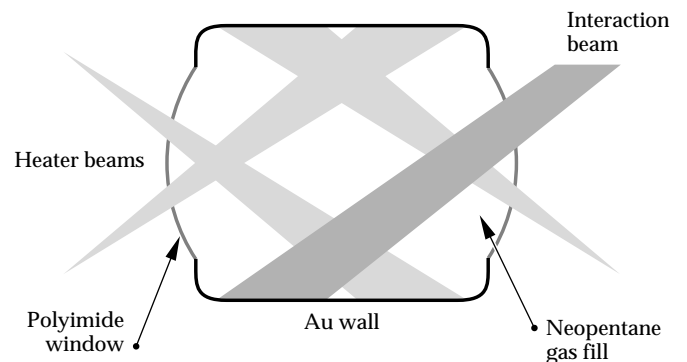


FIGURE 1. Schematic diagram of the target geometry. Shaded regions show the focusing and pointing of the heater beams (light shading) and interaction beam (dark shading). (10-01-0395-0652pb01)

absorption length exceeds the target size for the temperatures of interest (>5 mm for $0.351\text{-}\mu\text{m}$ light at $T_e = 3$ keV), the energy absorbed in the gas is determined by the laser-path length. The heater beam geometry (shown in Fig. 1) has the long path length necessary to maximize the absorption in the gas and to produce the desired plasma temperature. We also use a ramped pulse for the heater beams, which keeps the initial intensities low, to minimize scattering from the solid window material or the initially cold fill gas.

The detailed plasma conditions for the Nova gas-filled hohlraums and NIF targets are obtained from two-dimensional LASNEX¹² simulations. The simulations are cylindrically symmetric about the hohlraum axis and include the Au hohlraum wall, the gas fill (including dopants in the Nova targets), the membrane over the laser entrance hole (LEH) which confines the gas, and (in the case of the NIF target) the capsule. Standard LASNEX models are used for Lagrangian hydrodynamics, laser absorption, electron and radiation transport, and nonequilibrium atomic physics. The simulations predict that a uniform plasma (~ 2 mm long) with $n_e \sim 10^{21}\text{cm}^{-3}$, $T_e \sim 3$ keV, and flow velocity $<10^7\text{cm/s}$ is maintained for longer than 0.5 ns during the peak of the interaction pulse. Under these conditions, the small signal intensity gain coefficient for SBS is

$$G_{\text{SBS}} = \pi \times 10^{-16} \left(\frac{I^2}{T_e} \right) \left(\frac{n_e}{n_c} \right) \left(\frac{\omega_a}{v_i} \right) \left(\frac{L}{\lambda} \right), \quad (1)$$

where λ is the laser wavelength and L is the plasma length, both in micrometers; T_e is in keV; ω_a and v_i are the ion-acoustic-wave frequency and amplitude damping rate, respectively; and I is in W/cm^2 .

To illustrate the similarity between plasma conditions in NIF target designs and these Nova gas-filled hohlraums, Table 1 summarizes the SBS gain and the calculated values of the plasma parameters in the underdense plasma that determine the gain.

The Nova plasma parameters are within $\sim 50\%$ of the NIF values except for the T_i/T_e ratio (where T_i is the ion temperature), which is lower in the Nova targets

due to the shorter time available for electron-ion equilibration to occur. This difference leads to larger ion acoustic wave damping v_i in NIF than in Nova targets.² However, the difference in path length compensates to give similar gain coefficients for NIF and Nova targets at the same intensity ($I \cong 2 \times 10^{15} \text{ W/cm}^2$). Hence, these Nova targets access conditions that are very similar to NIF designs both in SBS linear gain and in the individual plasma parameters that determine the scattering characteristics. Calculated gain coefficients for the highest-intensity Nova experiments ($I \cong 5 \times 10^{15} \text{ W/cm}^2$) exceed the NIF value by more than a factor of two.

We performed extensive characterization to assure that predicted plasma conditions were achieved in the underdense plasma. The T_e is inferred from both single-element and isoelectronic line ratios¹³ using Ti/Cr or K/Cl spectra from thin foils placed in the path of the interaction beam. In the isoelectronic technique, one looks at x rays emitted from different ions, which contain the same number of electrons (e.g., x rays from Ti and Cr ions that each contain one electron ‘‘H-like’’). The ratio of the x-ray intensity from these differing ions is temperature dependent, but is nearly independent of other parameters, such as density.¹³ This makes the analysis and interpretation of the data more straightforward. Detailed analysis of the isoelectronic spectra confirms that $T_e > 3$ keV during the interaction pulse.¹⁴ Time-resolved measurements without the interaction beam verify that electron conduction provides good temperature uniformity. Several diagnostics characterize the propagation of the heating beams through the (initially) cold gas. A streaked x-ray spectrometer records the temporal history of Au M-band x rays emitted through the LEH. This measures the time at which the laser beam begins to heat the Au wall of the hohlraum; from this data, we can deduce the average beam propagation speed through the gas. Time-gated ($\cong 100$ ps) x-ray images, dominated by emission from 1% Ar dopant in the gas, provide evidence that the beams propagate without significant breakup or refraction. These experimental observations, which are in good agreement with LASNEX predictions, support important aspects of our modeling of NIF targets.

SBS Data and Discussion

Backscattered light near the laser frequency is collected by the interaction beam focusing lens and is measured with a grating spectrometer-streak camera combination to provide spectrally and temporally resolved data. The resolutions are 0.1 nm (spectral) and 100 ps (temporal). We also use time-integrating

TABLE 1. Comparison of selected plasma parameters for Nova gas-filled hohlraums and NIF targets.

	Nova	NIF
Interaction length	~ 2 mm	~ 3 mm
Line density $\int (n_e/n_c) dl$	~ 0.2 mm	~ 0.3 mm
T_e	3 keV	5 keV
T_i/T_e ratio	0.1–0.2	0.4
Gain coefficient G_{SBS} ($2 \times 10^{15} \text{ W/cm}^2$)	22	21

calorimeters to provide an absolute calibration. Figure 2 shows a typical spectrum. Just after time zero, before the interaction (or “probe”) beam is turned on, weak sidescattered light is observed from the “heater” beams as they interact with the polyimide window. At 0.6 ns, the “probe” beam is turned on; its reflection from the expanding polyimide window at the LEH produces the unshifted feature observed to start at 0.6 ns. A stimulated Raman scattering diagnostic (not shown) observes $\omega/2$ scattered light (700 nm) at this time; since half-harmonic light is generated at the $n_c/4$, this confirms the LASNEX prediction that the expanding window plasma density is still over $n_c/4$ when the probe beam is first turned on. However, it quickly drops below the gas density of $0.1 n_c$, and red-shifted SBS is then observed. This SBS backscatter (shown in Fig. 2) peaks soon after the interaction beam reaches peak intensity and decreases before the intensity drops. We calculate that the decrease is due to an increase in the ion acoustic wave damping rate, as the ratio of T_i/T_e increases. The time dependence of this ratio is due to the relatively slow heating of the ions; the ion heating depends on electron-ion collisions, which are relatively weak for low-Z plasmas. At the time of peak scattering, the wavelength of the peak emission is red-shifted $\sim 3\text{--}7 \text{ \AA}$. In the fluid limit, the frequency shift of SBS-scattered light $\Delta\omega = 2 k_0 (V_{||} - C_s)$, where k_0 is the laser wavenumber, C_s is the ion sound speed, and $V_{||}$ is the flow velocity parallel to the scattering vector; hence the observed red-shift is evidence that the SBS

spectrum is dominated by scattering from regions of plasma where $V_{||} < C_s$, as predicted by linear gain analysis. In contrast, SBS spectra from lower-temperature, expanding targets⁴ are routinely blue-shifted.

Figure 3 shows the peak SBS backscatter into the lens as a function of intensity for $f/4$ and $f/8$ interaction beams (using an RPP smoothed interaction beam). Peak SBS reflectivities with $f/8$ interaction beams, which closely match the NIF beam configuration, are $<3\%$ for C_5H_{12} -filled targets. Time-integrated reflectivities are $<1\%$. The scattering levels for all intensities are well below the $>30\%$ reflectivities predicted by linear theory. Reflectivity levels are not changed when four-color bandwidth is added. This insensitivity to bandwidth agrees with simulations¹⁰ only if ad hoc nonlinear damping rates are imposed to match the measured SBS reflectivity. At higher interaction intensities ($>2 \times 10^{15} \text{ W/cm}^2$), the simulations indicate that filaments form and scatter significant light outside the lens cone. Experiments are planned to investigate the angular distribution of the reflected light.

Peak scattering levels from $f/4$ interaction beams are comparable to the $f/8$ beams (1–2%). With SSD bandwidth of 3.5 \AA , scattering from the interaction beam is below the detection threshold of $\sim 0.1\%$. The apparent efficiency of SSD in suppressing SBS may be related to the details of the speckle motion: with SSD, the hot spots move in an effectively random way, whereas with four-color smoothing the hot spot pattern exactly recurs in a time $2\pi/\delta\omega$, where $\delta\omega$ is the line separation.

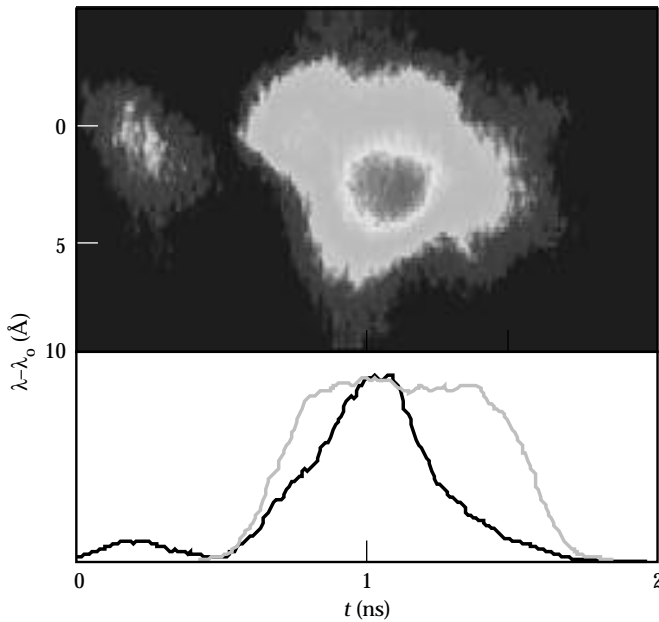


FIGURE 2. Streaked spectrum of backscattered light from the $f/8$ interaction beam. The plot shows temporal lineouts of the frequency-integrated reflectivity (black line) and the interaction beam intensity (gray line). The peak reflectivity is 0.015 and the peak intensity is $I = 1.7 \times 10^{15} \text{ W/cm}^2$. (10-01-0395-0653pb01)

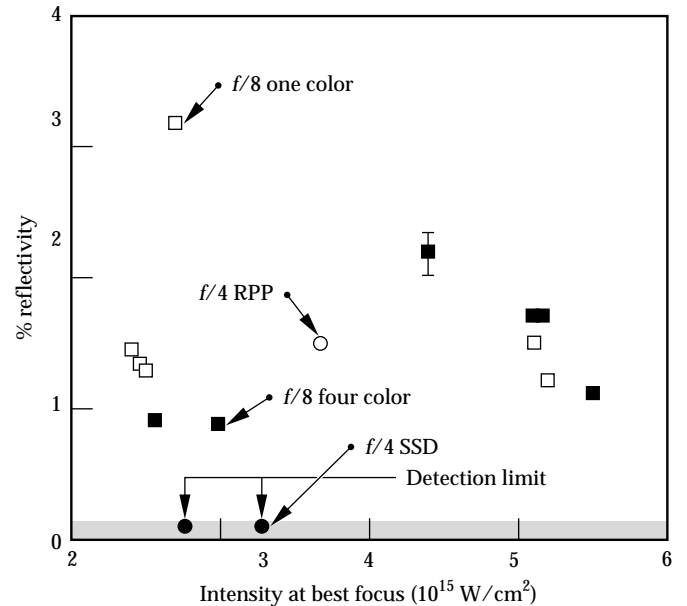


FIGURE 3. Peak SBS reflectivity into the focusing lens for $f/4$ and $f/8$ interaction beams, for an RPP-smoothed interaction beam. Filled squares show $f/8$ shots, adding four-color bandwidth with 4.4-\AA line separation. Reflectivities from $f/4$ shots with 3.5-\AA SSD bandwidth (filled circles) were below the detection threshold. (10-01-0395-0654pb01)

The observation of similar reflectivities from single-color $f/4$ and $f/8$ interaction beams at comparable intensities is somewhat at odds with gain scaling calculations. For these large plasmas, beam divergence produces a significant drop in intensity (a factor of ~ 2 for $f/8$ and ~ 4 for $f/4$) across the scattering region. This difference leads to larger calculated gain for $f/8$ ($G_{\text{SBS}} = 22$) than for $f/4$ ($G_{\text{SBS}} = 15$) for the same intensity at best focus. Several possible explanations for these findings are under investigation, theoretically and experimentally. For example, for the large gains calculated for these targets, nonlinear saturation mechanisms may limit the amplitude of the ion waves driven by SBS.³

High Levels of SBS

We observed only low levels of SBS when approximately duplicating the expected NIF conditions. We used several Nova shots with $f/4$ focusing to see if truly significant levels of energy could be scattered at more extreme conditions. We found that, with the maximum Nova power, we could generate a high level of SBS by removing all beam smoothing, and simultaneously removing H ions from the target. With no beam-smoothing techniques employed, the interaction intensity is difficult to define, making comparison with theory difficult. The spot size continually increases as the beam propagates from best focus, through the LEH, through the gas, to the Au wall. Furthermore, the unsmoothed Nova beams contain a substantial fraction of their energy in localized regions of high intensity.

Ions of H are particularly adept at damping the ion-acoustic waves. Their low mass means that, at a given temperature, their thermal velocities are higher than those of more massive ions, and thus they are more closely matched to the ion-acoustic wave's phase velocity. This enables them to draw energy away from the wave, effectively damping it. To remove H from the target, we used deuterated C_5D_{12} gas.

Figure 4 shows the resulting time-resolved SBS spectrum from this shot. Its features illustrate brief,

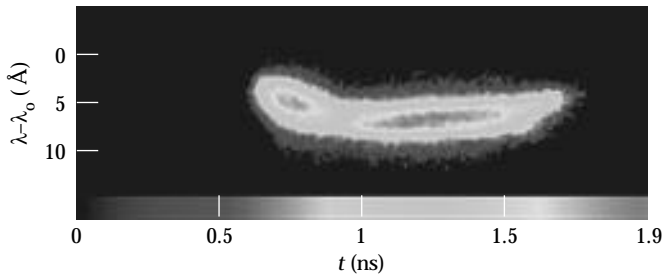


FIGURE 4. Streaked spectrum of backscattered light from the $f/4$ interaction beam with no smoothing and from the fully deuterated C_5D_{12} gas target. In contrast to Fig. 2, the reflectivity is nearly 20% and persists throughout the interaction pulse. (10-01-0395-0655pb01)

nearly unshifted scatter from the window-plasma when the probe beam turns on followed by red-shifted SBS. Unlike the data shown in Fig. 2, taken with smoothed beams, the SBS persists throughout the probe pulse. This shows that the (non-H) ions, in this case, are ineffective at damping the acoustic wave. Also unlike the smoothed beam data, the scattering level is high. In this case, 18% of the probe energy was scattered back into the $f/4$ lens.

Partially as a result of these experiments, the NIF target design now includes a small amount of H gas in the hohlraum to add an increased safety margin to the suppression of SBS.

Summary

We demonstrated low SBS reflectivity in NIF-relevant gas-filled hohlraum experiments on Nova. These targets approximately produced the calculated plasma conditions and SBS gain coefficients for NIF targets. The interaction beam mimics the NIF laser beam intensity, focusing, and beam smoothing. The maximum time-dependent SBS reflectivity is less than 3% for NIF-relevant conditions.

Acknowledgments

The authors thank J. Kilkenny, J. Lindl, and M. Rosen of Lawrence Livermore National Laboratory; and J. Fernandez, W. Hsing, and B. Wilde of Los Alamos National Laboratory. The contributions of the Nova laser operations and target fabrication groups were indispensable in conducting these experiments. Polyimide membranes were fabricated by Luxell, Inc. We acknowledge the LASNEX group for the simulations required to design and analyze these experiments.

Notes and References

1. S. W. Haan, S. M. Pollaine, J. D. Lindl, L. J. Suter, et al., "Design and Modeling of Ignition Targets for the National Ignition Facility," Lawrence Livermore National Laboratory, Livermore, CA, UCRL-JC-117034; submitted to *Phys. of Plasmas*.
2. E. A. Williams, R. L. Berger, A. M. Rubenchik, R. P. Drake, et al., *Phys of Plasmas* 2, 129 (1995).
3. W. L. Kruer, *Phys. Fluids* 23, 1273 (1980).
4. H. A. Baldis, D. S. Montgomery, J. D. Moody, C. Labaune, et al., *Plasma Phys. Controlled Fusion* 34, 2077 (1992) and refs. therein.
5. Y. Kato and K. Mima, *Appl. Phys. B* 29, 186 (1982).
6. S. Skupsky, R. W. Short, T. Kessler, R. S. Craxton, et al., *Appl. Phys.* 66, 3456 (1989).
7. S. N. Dixit, I. M. Thomas, B. W. Woods, A. J. Morgan, et al., *Applied Optics* 32, 2543 (1993).
8. A. J. Schmitt, *Phys. Fluids* 31, 3079 (1988).
9. R. L. Berger, B. F. Lasinski, T. B. Kaiser, E. A. Williams, et al., *Phys. Fluids B* 5, 2243 (1993).
10. R. L. Berger, *Bull. Am. Phys. Soc.* 38, 2012 (1993).

11. This target geometry is one of three simultaneous and complementary experiments performed on Nova, using gas-filled targets to create large-scale-length plasmas. Experiments using targets in which the gas is contained in a low-Z membrane are reported by B. J. MacGowan et al., *Proceedings of the IAEA 15th Int'l Conference on Plasma Physics and Controlled Nuclear Fusion Research*, IAEA-CN-60, 1994. An alternate hohlraum geometry was fielded by a team from Los Alamos National Laboratory led by J. Fernandez.
12. G. Zimmerman and W. Kruer, *Comments Plasma Phys. Controlled Fusion* 2 85 (1975).
13. R. S. Majoribanks, M. C. Richardson, P. A. Jaanimagi, R. Epstein, *Phys. Rev. A* 46, 1747 (1992); T. D. Shepard, C. A. Back, B. H. Gailor, W. W. Hsing, et al., *ICF Quarterly Report* 4(4) 137, Lawrence Livermore National Laboratory, Livermore, CA, UCRL-LR-105821-94-4 (1994).
14. C. A. Back, Lawrence Livermore National Laboratory, Livermore, CA, private communication regarding electron temperature measurements in laser heated hohlraums (1995); to be published later in a journal article.